

ORIGINAL RESEARCH

Myocardial Work in Patients Hospitalized With COVID-19: Relation to Biomarkers, COVID-19 Severity, and All-Cause Mortality

Flemming Javier Olsen , MD; Mats Christian Højbjerg Lassen , MD; Kristoffer Grundtvig Skaarup , MD; Jacob Christensen , BSc; Filip Soeskov Davidovski , BSc; Alia Saed Alhakak, MD, PhD; Morten Sengeløv, MD; Anne Bjerg Nielsen , BSc; Niklas Dyrby Johansen , MD; Claus Graff, PhD; Henning Bundgaard , MD, DMSc; Christian Hassager , MD, DMSc; Reza Jabbari, MD, PhD; Jørn Carlsen , MD, DMSc; Ole Kirk, MD, DMSc; Matias Greve Lindholm, MD, PhD; Lothar Wiese, MD, PhD; Ole Peter Kristiansen, MD, DMSc; Olav W. Nielsen , MD, DMSc; Birgitte Lindegaard, MD, PhD; Niels Tønder, MD, DMSc; Charlotte Suppli Ulrik , MD, DMSc; Morten Lamberts , MD, PhD; Pradeesh Sivapalan, MD, PhD; Gunnar Gislason , MD, PhD; Kasper Iversen , MD, DMSc; Jens Ulrik Stæhr Jensen , MD, PhD; Morten Schou , MD, PhD; Jesper Hastrup Svendsen , MD, DMSc; John Moene Aalen, MD, PhD; Otto Armin Smiseth, MD, PhD; Espen Wattenberg Remme, PhD; Tor Biering-Sørensen , MD, PhD, MPH

BACKGROUND: COVID-19 infection has been hypothesized to affect left ventricular function; however, the underlying mechanisms and the association to clinical outcome are not understood. The global work index (GWI) is a novel echocardiographic measure of systolic function that may offer insights on cardiac dysfunction in COVID-19. We hypothesized that GWI was associated with disease severity and all-cause death in patients with COVID-19.

METHODS AND RESULTS: In a multicenter study of patients admitted with COVID-19 (n=305), 249 underwent pressure-strain loop analyses to quantify GWI at a median time of 4 days after admission. We examined the association of GWI to cardiac biomarkers (troponin and NT-proBNP [N-terminal pro-B-type natriuretic peptide]), disease severity (oxygen requirement and CRP [C-reactive protein]), and all-cause death. Patients with elevated troponin (n=71) exhibited significantly reduced GWI (1508 versus 1707 mmHg%; $P=0.018$). A curvilinear association to NT-proBNP was observed, with increasing NT-proBNP once GWI decreased below 1446 mmHg%. Moreover, GWI was significantly associated with a higher oxygen requirement (relative increase of 6% per 100-mmHg% decrease). No association was observed with CRP. Of the 249 patients, 37 died during follow-up (median, 58 days). In multivariable Cox regression, GWI was associated with all-cause death (hazard ratio, 1.08 [95% CI, 1.01–1.15], per 100-mmHg% decrease), but did not increase C-statistics when added to clinical parameters.

CONCLUSIONS: In patients admitted with COVID-19, our findings indicate that NT-proBNP and troponin may be associated with lower GWI, whereas CRP is not. GWI was independently associated with all-cause death, but did not provide prognostic information beyond readily available clinical parameters.

REGISTRATION: URL: <https://www.clinicaltrials.gov>; Unique identifier: NCT04377035.

Key Words: corona ■ COVID ■ myocardial work ■ pressure-strain

Correspondence to: Flemming Javier Olsen, MD, Cardiovascular Non-Invasive Imaging Research Laboratory, Department of Cardiology, Herlev and Gentofte Hospital, University of Copenhagen, Denmark, Gentofte Hospitalsvej 1, 2900 Hellerup, Denmark. Email: flemming.j.olsen@gmail.com

Supplemental Material is available at <https://www.ahajournals.org/doi/suppl/10.1161/JAHA.122.026571>

For Sources of Funding and Disclosures, see page 13.

© 2022 The Authors. Published on behalf of the American Heart Association, Inc., by Wiley. This is an open access article under the terms of the [Creative Commons Attribution-NonCommercial-NoDerivs](https://creativecommons.org/licenses/by-nc-nd/4.0/) License, which permits use and distribution in any medium, provided the original work is properly cited, the use is non-commercial and no modifications or adaptations are made.

JAHA is available at: www.ahajournals.org/journal/jaha

CLINICAL PERSPECTIVE

What Is New?

- Myocardial work is associated with biomarkers suggestive of myocardial injury in patients admitted with COVID-19.
- Myocardial work is associated with oxygen requirement as a sign of COVID-19 severity.
- Myocardial work is associated with all-cause death in patients with COVID-19.

What Are the Clinical Implications?

- The findings indicate that a novel echocardiographic measure of systolic function (ie, myocardial work) is associated with myocardial injury and disease severity in COVID-19 but does not improve risk prediction of all-cause mortality.
- Future studies should validate our findings and explore the potential of myocardial work for predicting cardiovascular outcomes.

Nonstandard Abbreviations and Acronyms

EWS	early warning score
GCW	global constructive work
GLS	global longitudinal strain
GWE	global work efficiency
GWI	global work index
GWW	global wasted work
PSL	pressure-strain loop

Cardiovascular disease is a frequently encountered comorbidity in patients admitted with COVID-19, and studies suggest that preexisting cardiovascular disease increases the risk of both major adverse cardiovascular events and in-hospital mortality.¹⁻³ Although COVID-19 infection can induce a systemic inflammation, resulting in cardiac complications, it may also affect left ventricular (LV) function through various other mechanisms.^{4,5} Accordingly, biomarker-based studies suggest that COVID-19 is frequently associated with cardiac injury (defined as elevated troponin) and that presence of cardiac injury, in turn, poses an increased risk of death.⁶

Given the high frequency of cardiac involvement and cardiac complications observed with COVID-19,² there is a need for improving our understanding of how COVID-19 infection affects the myocardium and the clinical relevance of myocardial dysfunction in COVID-19. Novel echocardiographic techniques hold potential for detecting myocardial abnormalities and may thereby help delineate the mechanism by which

COVID-19 affects LV function. It may furthermore identify patients at risk of a poor disease course to help tailor patient management and improve prognosis. Several echocardiographic studies have been performed in patients with COVID-19, and these have persistently shown that right ventricular (RV) dysfunction is an important marker of mortality risk.⁷⁻¹⁰ Although several studies have also shown an association between LV global longitudinal strain (GLS) and clinical outcomes in patients with COVID-19,^{8,10} others have reported that this association is influenced by the presence of hypertension, owing to the afterload dependency of GLS.¹¹

An extension of myocardial speckle tracking has recently been introduced, the so-called pressure-strain loop (PSL) analyses.¹² PSL contemplates the use of blood pressure (BP) and valvular event timing in conjunction with LV speckle tracking to provide pressure-strain area curves that can quantify the amount of myocardial work, the global work index (GWI), performed by the LV.¹² Consequently, it incorporates afterload and, therefore, provides a more valid measure of intrinsic myocardial contractile function than with strain imaging. GWI has also shown to correlate closely with LV metabolism and may, therefore, be a useful marker in ischemic heart disease.¹² In addition, PSL analyses also acquire measures of paradoxical deformation that have been reported as useful markers in myocardial ischemia.¹³ Taken together, PSL analyses may, therefore, be useful in patients with COVID-19 given the high prevalence of cardiac injury that could suggest presence of myocardial ischemia.

Therefore, we hypothesized that GWI was associated with cardiac and inflammatory biomarkers, COVID-19 severity, and all-cause death and investigated this in a detailed, prospective, echocardiographic study of patients admitted with COVID-19. Because PSL analyses can also quantify constructive work, wasted work, and work efficiency, which reflect the amount of paradoxical motion that may develop with cardiac injury, secondary to myocardial ischemia, we also explored how these myocardial work indexes relate to the above-mentioned factors.

METHODS

Data Availability

The data cannot be shared publicly because they contain sensitive information on study participants. This is in line with Danish regulations. Request for data access should be directed to the Danish Data Protection Agency (“Videnscenter for Dataanmeldelser”).

Study Population

The study is an analysis based on the ECHOVID-19 study, a multicenter study of patients admitted with

laboratory-confirmed COVID-19 during the 2 Danish COVID-19 epidemic waves. The study included patients admitted at any hospital located in the eastern part of Denmark, comprising a total of 8 centers. Patients were included from COVID-19 wards but not intensive care units. Patients were included independently of their clinical and health profiles. Inclusion for the first wave spanned from March 30 through June 3, 2020 (n=215), and the second wave spanned from January 19 through March 12, 2021 (n=90), resulting in a total of 305 patients. Details on viral strains were not specifically investigated in this study; however, the dominant viral strain during the first wave was the 20C clade, and the dominant viral strains during the second wave were the 20E (EU1) and Alpha (B.1.1.7).

PSL analysis assumes that BP may be used as a noninvasive surrogate of LV pressure. This assumption is not fulfilled in patients with outflow obstruction, patients were excluded if they had any degree of aortic valve stenosis (n=11), leaving 294 eligible for analyses. Of these, 1 patient was excluded because of missing details on BP and 44 patients were excluded because of insufficient image quality for speckle tracking and valvular event timing analyses, leaving 249 for final analyses. An overview of the inclusion process and data availability is shown in [Figure 1](#). The study was registered at [Clinicaltrials.gov](#) (identifier: NCT04377035) and was approved by the regional scientific ethics committee (identifier: H-20021500). Informed consent was obtained from all patients, and the study adhered to the second Declaration of Helsinki.

Baseline Information

Details on medical history and current medication were obtained by a questionnaire and from electronic medical health records. Vital signs (BP, heart rate, temperature, respiratory frequency, and oxygen saturation) were acquired at the time of the echocardiogram and were used to calculate the early warning score (EWS). Venous blood samples were drawn at the time of the echocardiogram and included measurement of plasma values for NT-proBNP (N-terminal pro-B-type natriuretic peptide) (available in 162) and troponin I and troponin T (available in 86 and 88, respectively), creatinine (available in 247), and CRP (C-reactive protein) (available in 241). For analysis of NT-proBNP, patients with a creatinine of $>150 \mu\text{mol/L}$ were excluded because of unreliable NT-proBNP values (n=20). Myocardial injury was defined as elevated troponin, defined as either troponin I or troponin T above the institutional 99th percentile. Known heart disease was defined as presence of either ischemic heart disease or heart failure. A more detailed outline of the definition of comorbidities has previously been published and is available in [Data S1](#).^{8,14}

Outcome

The primary outcome was all-cause death, obtained from medical records. End point extraction was made on June 17, 2020, for the first wave, and on April 15, 2021, for the second wave. At this point, no patient was any longer admitted. In addition, secondary outcomes included cardiac biomarkers (elevated troponin and NT-proBNP) and COVID-19 severity, assessed by oxygen requirement and CRP.

Echocardiography

Bedside transthoracic examinations were performed in all patients according to a prespecified protocol using a portable ultrasound machine (Vivid IQ; GE Healthcare, Horten, Norway). The median time between admission and echocardiography was 4 days (interquartile range, 2–8 days). The examinations were stored in a remote digital archive (Viewpoint 6.11.2), and echocardiographic analyses were performed as postprocessing analyses with commercially available software (EchoPAC 203; GE Healthcare).

Conventional echocardiographic measurements were performed according to the 2015 European Association of Cardiovascular Imaging/American Society of Echocardiography recommendations for cardiac chamber quantification,¹⁵ and a detailed description of the analyses is provided in [Data S1](#). Reduced LV ejection fraction (LVEF) was defined as an LVEF $<52\%$ for men and $<54\%$ for women. RV systolic dysfunction was defined as a tricuspid annular plane systolic excursion $<17 \text{ mm}$. RV hypertension was defined as present if the tricuspid regurgitant velocity was $>2.8 \text{ m/s}$. If this was not measurable, RV hypertension was instead defined on the basis of secondary indicators, according to pulmonary hypertension guidelines¹⁶ ([Data S1](#)).

PSL Analyses

The process of performing PSL analyses is shown in [Figure 2](#). Three key elements were acquired for PSL analyses: (1) Arterial cuff BP, measured at rest by an automatic BP monitor. (2) Valvular event timing, measured using color tissue Doppler images of the apical 4-chamber view by placing a curved M-mode sample through the anterior mitral valve leaflet. From a color-based scheme, the opening and closure of the aortic and mitral valve were then determined.¹⁷ (3) LV strain traces, obtained by myocardial speckle tracking performed in the apical 4-chamber view, 2-chamber view, and longitudinal long-axis view (mean frame rate, 55 ± 4 frames per second). Speckle tracking was performed with a semiautomatic approach, and segments that were persistently untraceable were excluded.

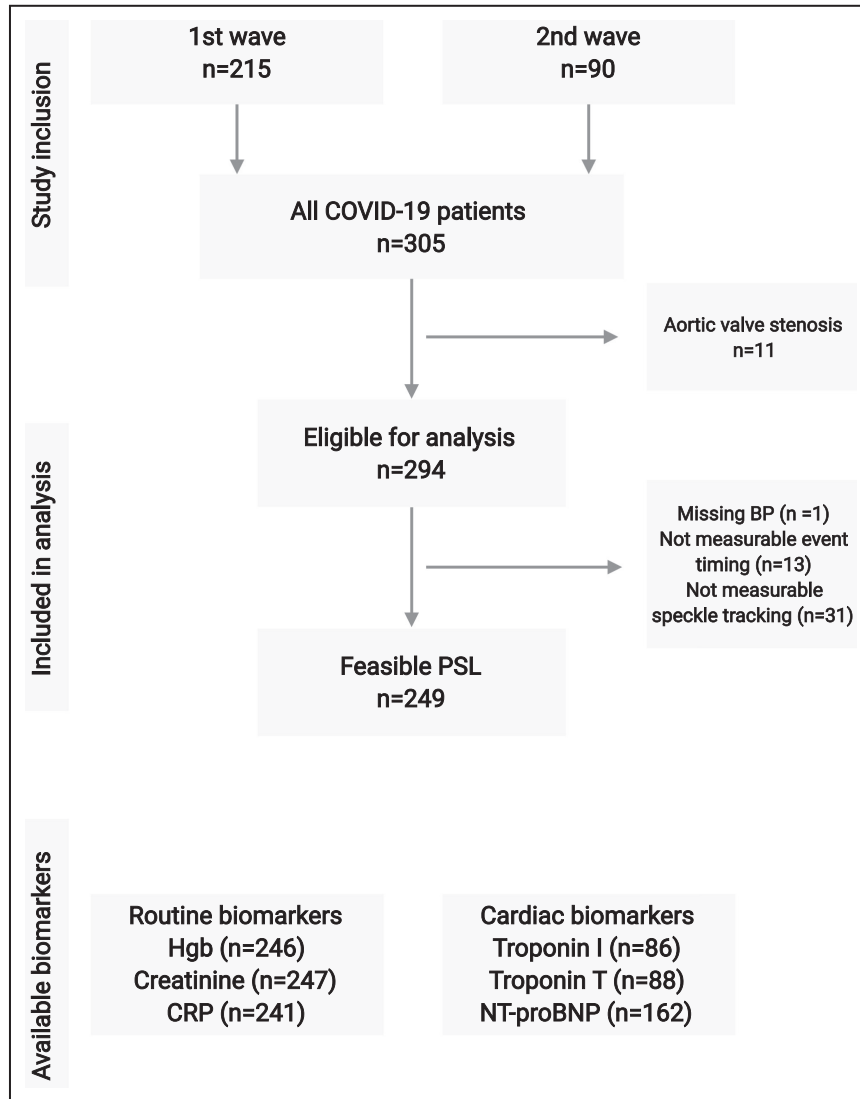


Figure 1. Flowchart.

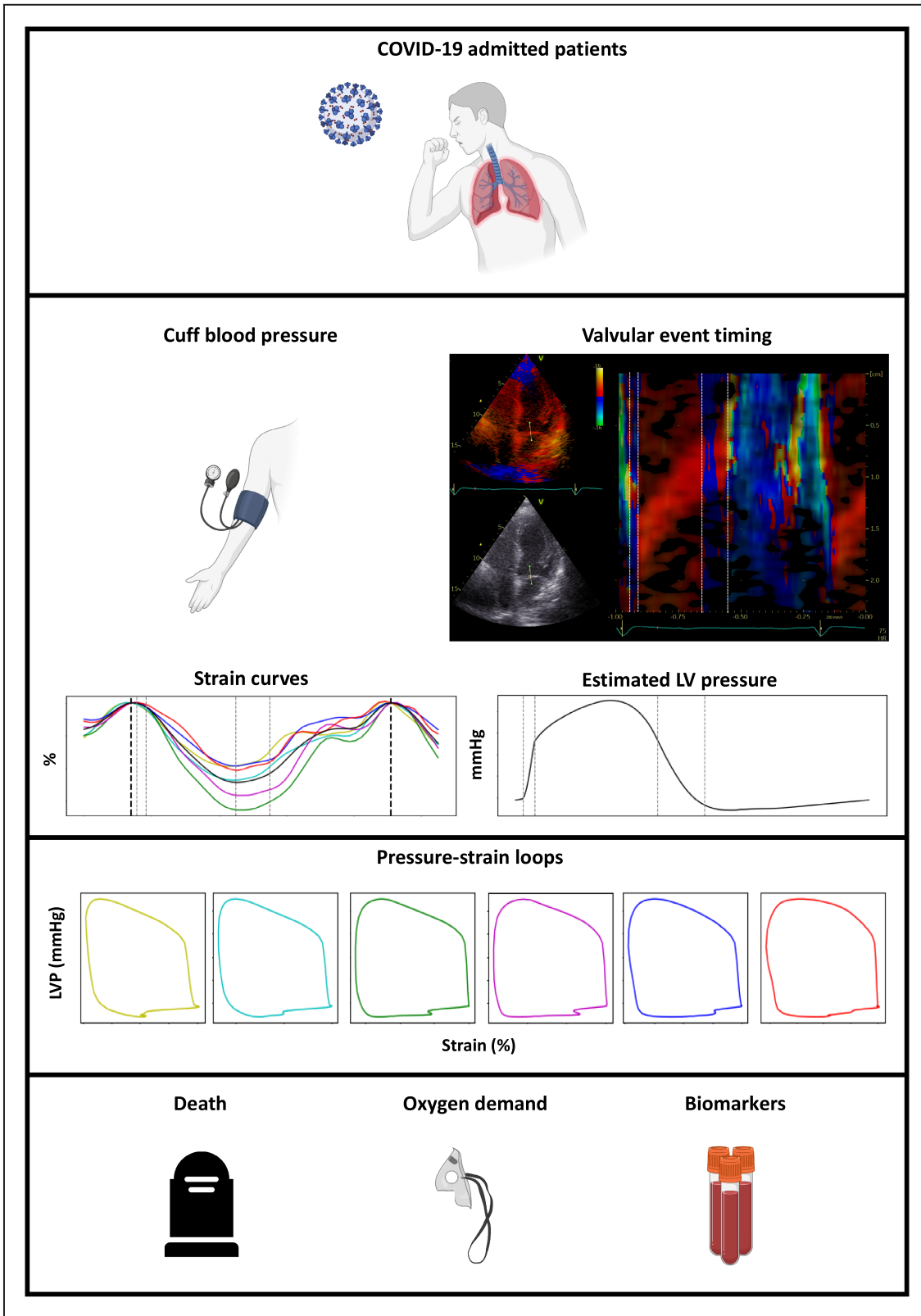
Flowchart showing study inclusion process and data availability. Created with [Biorender.com](https://biorender.com). BP indicates blood pressure; CRP, C-reactive protein; Hgb, hemoglobin; NT-proBNP, N-terminal pro-B-type natriuretic peptide; and PSL, pressure-strain loop.

Systolic BP and valvular event timings were used to customize a reference LV pressure curve to provide an individualized estimated LV pressure curve. Combined with strain traces, this estimated pressure curve was used to acquire segmental PSL. Global work indexes

were calculated as averages of segments. Because work represents the product of force (LV pressure in mmHg) and distance (strain in percentage), the unit for the work indexes is in mmHg%. The primary measure of interest was GWI, which represents the total

Figure 2. Overview of study methods and concept.

The figure summarizes the study design. Top panel: patients admitted with COVID-19 were included. Second panel: 4 steps in the pressure-strain loop analyses: (1) Arterial cuff blood pressure (BP) was measured. (2) Valvular event timing was measured by color tissue Doppler imaging M-mode. Color changes were used to place event timing. White dotted lines represent valvular event timings, as follows: from left to right on the figure: mitral valve closure, aortic valve opening, aortic valve closure, and mitral valve opening. (3) Strain curves were derived from left ventricular (LV) speckle tracking: each curve represents a myocardial segment from one projection. (4) An LV pressure (LVP) reference curve was customized according to valvular event timing and systolic BP to generate an estimated LVP curve, which, along with strain curves, were used to derive pressure-strain loops. Third panel: segmental pressure-strain loops, the area of which corresponds to the myocardial work index. Fourth panel: myocardial work index was then related to the outcomes of all-cause death and COVID-19 severity. Parts of the figure were created with [Biorender.com](https://biorender.com).



Downloaded from <http://ahajournals.org> by on February 14, 2023

work performed from mitral valve closure to mitral valve opening and consequently corresponds to the area within the PSL. Secondary exposure variables that were obtained included the following: global

constructive work (GCW), global wasted work (GWW), and global work efficiency (GWE). GCW represents the sum work from shortening during systole and lengthening during the isovolumic relaxation, and conversely

GWW represents the sum of work from lengthening during systole and shortening during isovolumic relaxation. GWE is calculated as the fraction of GCW to the sum of GCW and GWW.¹⁸

Abnormal work indexes were defined according to recently proposed age- and sex-stratified threshold values derived from the CCHS (Copenhagen City Heart Study) (Data S1).¹⁹

Statistical Analysis

For continuous variables, normality was assessed by histograms, and normally distributed variables are presented as means with SDs. Nonnormally distributed variables are presented as medians with interquartile ranges. Categorical variables are presented as total numbers and proportions. Clinical characteristics were compared across the 2 COVID-19 waves, between groups of PSL feasibility, and between groups with available versus non-available NT-proBNP. Groupwise comparisons of clinical and echocardiographic variables were further performed according to normal versus abnormal GWI, presence of myocardial injury, and all-cause mortality.

Linear regression analyses were performed to investigate the association between myocardial work indexes and NT-proBNP. Similar analyses were also performed to investigate the association between myocardial work indexes and CRP. Because of skewness, several variables were transformed to acquire normality. NT-proBNP and GWW were log transformed, CRP was square root transformed, creatinine was transformed with a 1/square root transformation, and GWE underwent a logit transformation. Multivariable adjustments were made for the following variables: age, sex, known heart disease, creatinine, and atrial fibrillation. These variables were selected because they are all associated with NT-proBNP and have also been linked to elevations in CRP.^{20–23}

Because a substantial part did not require supplemental oxygen, the oxygen requirement variable was overdispersed with excess zeros. Therefore, negative binomial regression analysis was applied for modeling for highly dispersed count data to investigate the association between myocardial work indexes and oxygen requirement. Multivariable adjustments were performed similar to the linear regression analyses.

Cox proportional hazards regression was used to examine the association between myocardial work indexes and all-cause death. Proportional hazards were examined by inspection of Schoenfeld residuals. Harrell's C-statistics were calculated from the univariable Cox regression analyses. Kaplan-Meier survival curves were constructed to illustrate the risk of all-cause death for abnormal versus normal work indexes throughout follow-up. The log-rank test was used to test for statistical significance across curves. Complementary loglog

survival plots were constructed to inspect proportionality for normal versus abnormal work indexes.

Multivariable Cox regression was made to adjust for confounders and obtain fitted hazard ratios (HRs). A limited number of covariates were selected to avoid overfitting. Adjustments were made for the most influential confounders, being well-established predictors of death and factors that would also influence myocardial work indexes. These included age, EWS, known heart disease, and left bundle-branch block by admission ECG. Test for interaction was made against age, sex, RV hypertension, and COVID-19 wave. Harrell's C-statistics were also calculated from multivariable Cox regression to explore whether work indexes or GLS would improve discrimination when added to a base model of age, EWS, and known heart disease. Comparative analyses of systolic measures were made by including GLS, LVEF, and work indexes sequentially in bivariable models (ie, LVEF and GWI in one model, and GLS and GWI in another model). Variance inflation factor was calculated as an estimate of collinearity.

Because of nonlinearity in some of the regression models, restricted cubic spline curves were created, and the number of knots was selected on the basis of the model that provided the lowest Akaike information criterion.

$P < 0.05$ was considered significant in all analyses.

All analyses were performed using STATA SE (version 15; StataCorp, College Station, TX).

RESULTS

Baseline clinical, biochemical, and echocardiographic characteristics are presented in Table 1. Briefly, the mean age was 68 ± 14 years, 57% were men, 15% had known heart disease, and the median EWS was 2 (interquartile range, 1–4).

In terms of echocardiographic characteristics, 21% had RV systolic dysfunction, 13% had RV hypertension, and 20% had LV systolic dysfunction by LVEF. Mean GWI was 1659 ± 550 mmHg%, mean GCW was 1852 ± 567 mmHg%, median GWW was 76 mmHg% (interquartile range, 48–130 mmHg%), and median GWE was 95.6% (interquartile range, 92.1%–97.5%). Table 1 also outlines clinical, biochemical, and echocardiographic characteristics, as stratified by normal versus abnormal GWI. Those with abnormal GWI were older, had a higher EWS, had lower BP, higher heart rate, more frequently had ischemic heart disease, heart failure, kidney dysfunction, and higher LV mass, and had reduced LV and RV systolic function.

Of note, no clinical differences were observed between patients in the 2 COVID-19 waves (Table S1). However, patients in whom PSL was feasible were younger (68 versus 73 years) than those without

Table 1. Baseline Characteristics for Entire Population and Stratified by GWI

Characteristic	All (n=249)	Normal GWI (n=143)	Abnormal GWI (n=106)	P value
Clinical				
Age, y	68±14	65±14	72±13	<0.001
Male sex	143 (57)	77 (54)	66 (62)	0.18
Body mass index, kg/m ²	27±5	27±5	26±5	0.09
Early warning score	2 (1–4)	2 (1–3)	3 (1–4)	<0.001
Systolic blood pressure, mmHg	127±19	132±19	119±17	<0.001
Diastolic blood pressure, mmHg	74±11	75±11	72±12	0.018
Heart rate, beats/min	81±16	78±14	85±18	<0.001
Oxygen saturation, %	95 (94–96)	95 (94–96)	95 (93–96)	0.22
Respiratory rate	18 (17–20)	18 (17–20)	19 (18–22)	0.14
Temperature, °C	37.0±0.69	37.0±0.70	37.1±0.68	0.96
Hypertension	131 (53)	68 (48)	63 (59)	0.06
Diabetes	62 (25)	35 (25)	27 (26)	0.91
Chronic obstructive pulmonary disease	33 (13)	17 (12)	16 (15)	0.46
Ischemic heart disease	26 (10)	10 (7)	16 (15)	0.039
Heart failure	25 (10)	4 (3)	21 (20)	<0.001
Biomarkers				
Plasma pro-B-type natriuretic peptide, ng/L	340 (118–1370)	304 (133–1036)	506 (118–1522)	0.36
Plasma troponin I, ng/L	12 (7–29)	11 (6–29)	14 (9–34)	0.32
Plasma troponin T, ng/L	21 (13–33)	18 (11–25)	25 (17–54)	0.008
Plasma CRP, mg/L	56 (23–95)	51 (20–85)	58 (24–98)	0.15
Plasma creatinine, μmol/L	75 (58–99)	70 (57–93)	81 (61–109)	0.042
Echocardiography				
Left ventricular mass index, g/m ²	82 (67–97)	78 (68–92)	90 (67–112)	0.045
Left ventricular internal diameter, cm	4.5±0.7	4.5±0.6	4.6±0.8	0.20
Left ventricular ejection fraction, %	59 (53–63)	61 (57–64)	53 (47–58)	<0.001
Left atrial volume, mL/m ²	20 (15–26)	20 (16–24)	22 (15–30)	0.10
Tricuspid annular plane systolic excursion, mm	20±4.8	22±4	18±5	<0.001
Tricuspid regurgitant gradient, mmHg	21±9	20±9	23±9	0.09
Right ventricular hypertension	32 (13)	15 (11)	17 (16)	0.20
Global longitudinal strain, %	–15.8±4.3	–18.3±2.8	–12.3±3.3	<0.001
Global constructive work, mmHg%	1852±567	2212±411	1366±341	<0.001
Global wasted work, mmHg%	76 (48–130)	68 (41–110)	88 (56–156)	0.003
Global work efficiency, %	95.6 (92.1–97.5)	96.7 (94.8–98.0)	92.2 (88.0–96.3)	<0.001

Continuous variables showing Gaussian distribution are shown as mean±SD. Continuous variables not showing Gaussian distribution are shown as median (interquartile range). Other data are given as number (percentage). CRP indicates C-reactive protein; and GWI, global work index.

feasible PSL analyses, and fewer had chronic obstructive pulmonary disease (13% versus 29%) (Table S2).

Association With Cardiac Biomarkers

Patients with abnormal GWI exhibited higher troponin T values compared with normal GWI but no difference for troponin I (Table 1). We did, however, observe that patients who had myocardial injury (n=71) exhibited significantly reduced GWI (1508 versus 1707 mmHg%; $P=0.018$) and GCW (1701 versus 1887 mmHg%; $P=0.026$), whereas no differences were observed for

GWW (81 mmHg% for both groups; $P=0.35$) nor GWE (95.1% versus 95.8%; $P=0.11$). These patients were also of older age, more frequently had hypertension and heart failure, and had a higher LV mass and lower LVEF (Table S3).

Patients with abnormal work indexes by GWI, GCW, and GWW did not exhibit any differences in NT-proBNP compared with those with normal work indexes. However, those with abnormal GWE did exhibit significantly higher NT-proBNP at baseline (median, 747 versus 290 ng/L; $P=0.006$, for abnormal versus

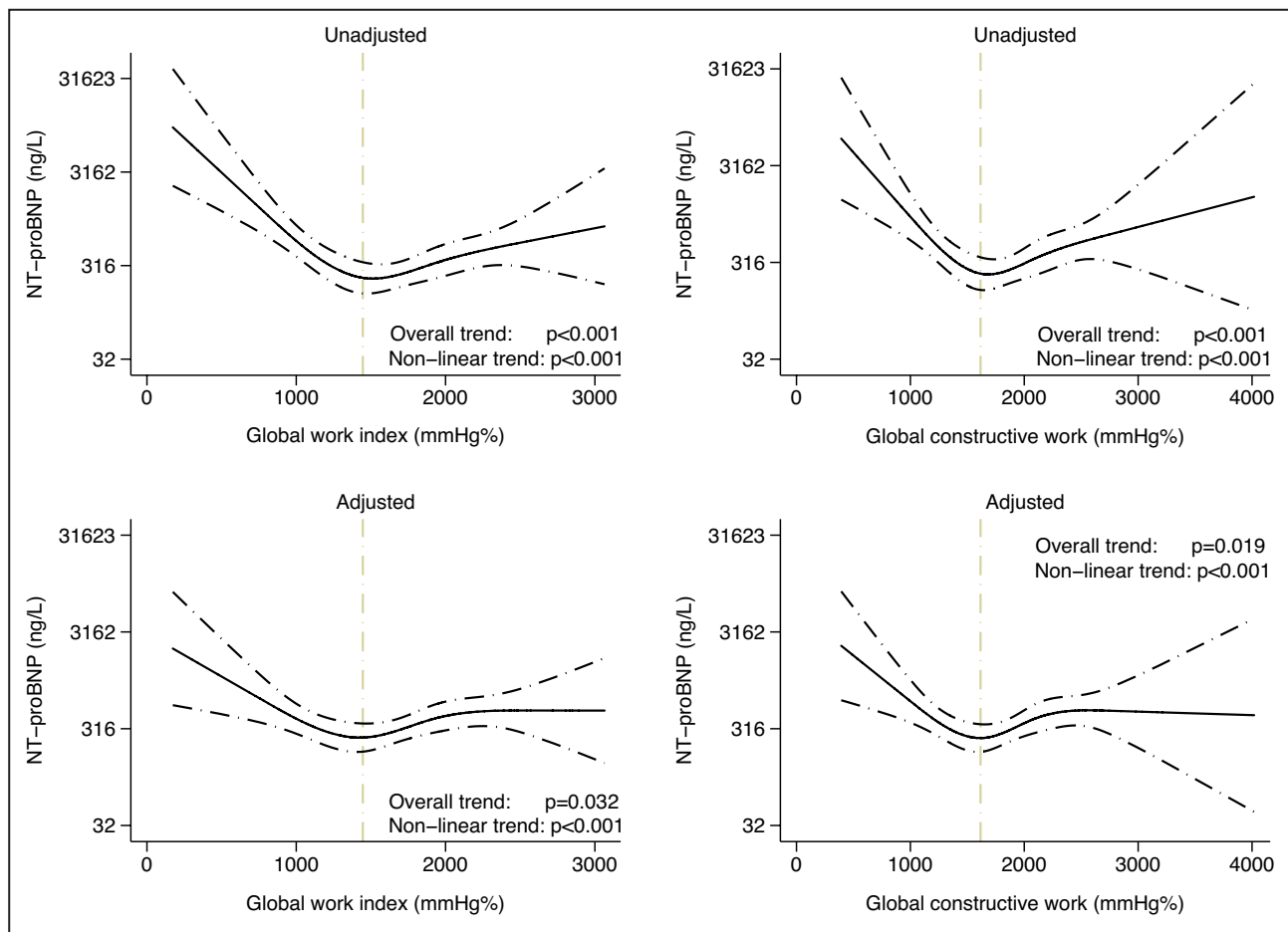


Figure 3. Association between work indexes and NT-proBNP (N-terminal pro-B-type natriuretic peptide).

The figures represent restricted cubic spline curves, showing a curvilinear association between global work index and NT-proBNP as well as global constructive work and NT-proBNP. In unadjusted models, both decreasing and increasing values of global work index beyond the inflection point of 1446 mmHg% were associated with increasing NT-proBNP (top left panel). A similar association can be appreciated for global constructive work and NT-proBNP (inflection point of 1616 mmHg%) (top right panel). After adjustments for relevant confounders, only decreasing values were associated with increasing NT-proBNP for both global work index (bottom left panel) and global constructive work (bottom right panel). The values of NT-proBNP are presented as geometric means.

normal GWE, respectively). Of note, patients who had NT-proBNP measured more frequently had heart failure at baseline (13% versus 5%; $P = 0.045$) than those who did not have NT-proBNP measured; otherwise, no clinical differences were observed (Table S4).

In unadjusted analyses, both GWI and GCW showed a significant curvilinear association with NT-proBNP (Figure 3A and 3B), but after multivariable adjustment, this association changed such that only decreasing GWI and GCW below the inflection points of 1446 and 1616 mmHg%, respectively, were associated with increasing NT-proBNP (Figure 3). No association with GWW and GWE was observed after multivariable adjustments.

Association With Severity of COVID-19

In linear regression analyses, no association was observed between any myocardial work indexes and

CRP, and patients with abnormal work indexes exhibited similar CRP levels as those with normal work indexes ($P > 0.05$ for all) (Figure S1).

At baseline, the patients who required any supplemental oxygen ($n = 138$) exhibited significantly reduced GWI and GCW (GWI: 1598 versus 1749 mmHg% [$P = 0.031$]; GCW: 1791 versus 1936 mmHg% [$P = 0.043$]), albeit similar GWW and GWE compared with those with normal work indexes. Decreasing GWI and GCW were associated with higher oxygen requirement (Figure 4A and 4B), which persisted after multivariable adjustments, showing a relative increase in oxygen requirement of 6% per 100-mmHg% decrease in both GWI and GCW (relative increase of 6% [95% CI, 1–11] [$P = 0.010$] and 6% [95% CI, 1–10] [$P = 0.011$] for GWI and GCW, respectively). No association between neither GWW nor GWE and oxygen requirement was observed after multivariable adjustments.

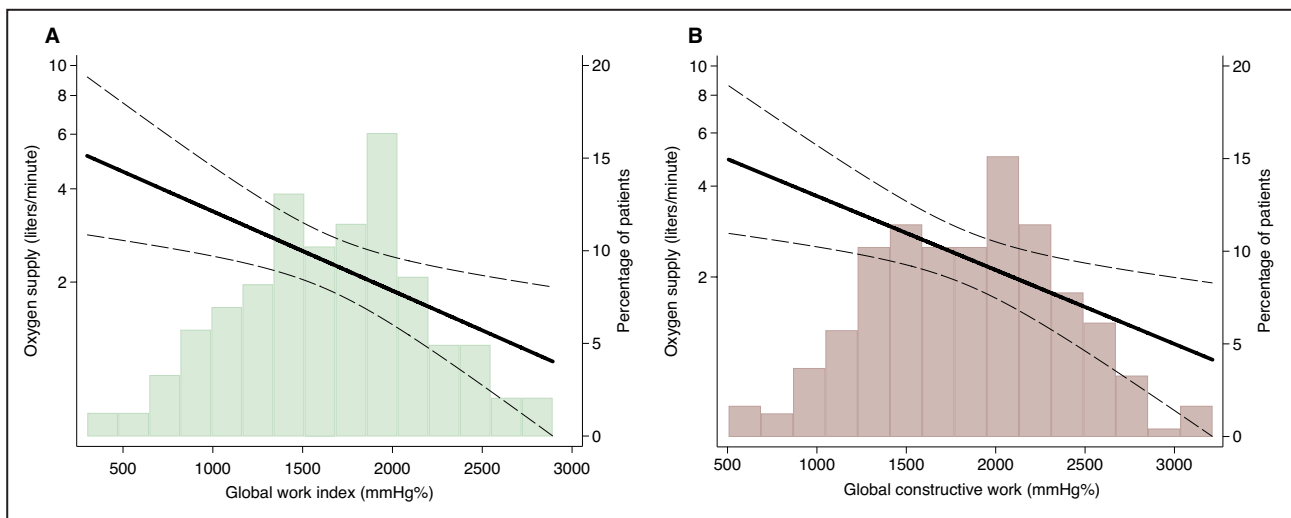


Figure 4. Association between work indexes and oxygen supply.

The figures represent unadjusted restricted cubic spline curves based on negative binomial regression analyses, showing that decreasing global work index (A) and global constructive work (B) were associated with increasing oxygen requirement. An underlying histogram is also provided, and the second y axis refers to this histogram.

Systolic Function and All-Cause Mortality

During a median follow-up of 58 days (interquartile range, 43–70 days), 37 (15%) died of any cause. Clinical, biochemical, and echocardiographic characteristics, stratified by survival status, are shown in Table S5.

The risk of dying with continuous changes in work indexes is shown in Figure 5. Furthermore, abnormalities in all work indexes were associated with a significantly increased risk of death, as shown in Figure 6.

After multivariable adjustment for age, EWS, known heart disease, and left bundle-branch block, GLS, GWI, GWW, and GWE remained significantly associated with all-cause death (Table 2). Of note, no effect modification was observed from age, sex, COVID-19 wave, or RV hypertension in multivariable models ($P > 0.05$ for interaction for all). In contrast, LVEF did not remain significantly associated with all-cause death after similar adjustments (HR, 1.03 [95% CI, 0.99–1.07] [$P = 0.11$], per 1% decrease).

Of all myocardial work indexes, GWI yielded the highest Harrell's C-statistic of 0.694, also higher than LVEF (C-statistic of 0.648) but similar to GLS (C-statistic of 0.697). However, neither GLS nor any of the work indexes significantly increased Harrell's C-statistics when added to age, EWS, and known heart disease (Harrell's C-statistic for age, EWS, and known heart disease: 0.778 versus age, EWS, known heart disease, and GWI: 0.790 [P for increment=0.39]; age, EWS, known heart disease, and GCW: 0.785 [P for increment=0.49]; age, EWS, known heart disease, and GWW: 0.791 [P for increment=0.24]; and age, EWS, known heart disease, and GWE: 0.788 [P for increment=0.44]).

In a bivariable model, including GWI and LVEF, only GWI remained significantly associated with all-cause death (GWI: HR, 1.14 [95% CI, 1.03–1.26] [$P = 0.012$], per 100–mmHg% decrease; LVEF: HR, 1.03 [95% CI, 0.99–1.07] [$P = 0.19$], per 1% decrease). The same was noted in a bivariable model with GLS and LVEF (GLS: HR, 1.15 [95% CI, 1.02–1.30] [$P = 0.028$], per 1% absolute decrease; LVEF: HR, 1.02 [95% CI, 0.97–1.07] [$P = 0.39$], per 1% decrease).

In a bivariable model including GWI and GLS, none of the 2 measures was associated with all-cause death. Variance inflation factor for this model was 3.06. Neither GCW nor GWE was associated with all-cause death in bivariable models with GLS, whereas GLS did remain associated with all-cause death in these models. However, this association for GLS did not persist with further multivariable adjustments (age, EWS, known heart disease, and left bundle-branch block). In a bivariable model with GLS and GWW, both variables were associated with all-cause death; however, only GWW remained associated with all-cause death with further multivariable adjustments (HR, 1.09 [95% CI, 1.00–1.18]; $P = 0.048$, per 50–mmHg% increase).

DISCUSSION

The key findings from this report can be summarized as follows: Cardiac dysfunction, as assessed by biomarkers, may be associated with reduced GWI and GCW, whereas inflammatory burden was not associated with any echocardiographic measure of myocardial function. Furthermore, GWI and GCW were also associated with disease severity by oxygen requirement, possibly

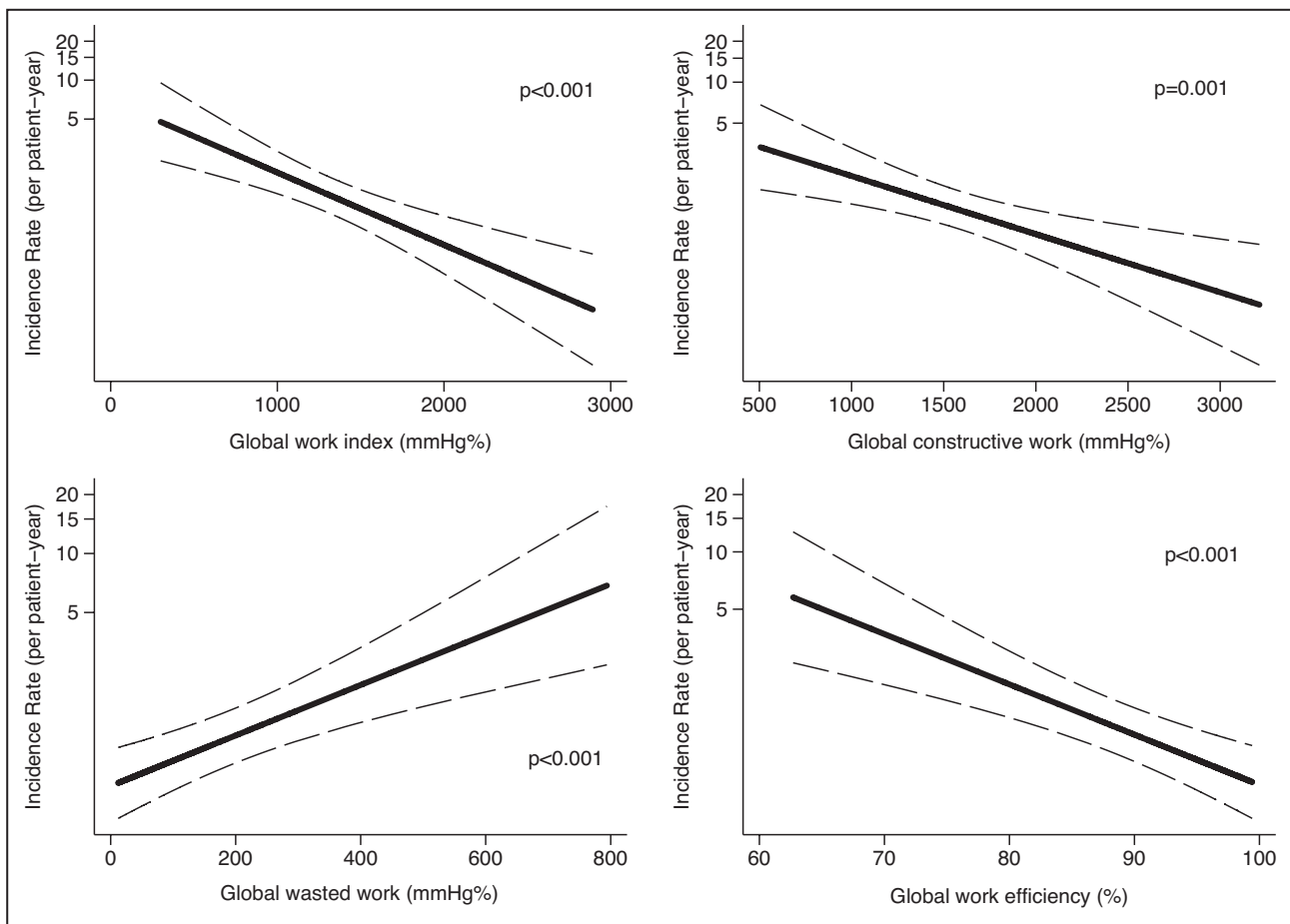


Figure 5. Association between work indexes and all-cause death.

The figures represent unadjusted restricted cubic spline curves based on Poisson regression, showing the continuous association between myocardial work indexes and the incidence rate of all-cause death. Decreasing global work index (top left panel), global constructive work (top right panel), and global work efficiency (bottom right panel) were all associated with a higher risk of all-cause death, and so was increasing global wasted work (bottom left panel).

reflecting their close association to myocardial oxygen consumption. Finally, we observed that GWI, GWW, and GWE were associated with all-cause death, but the measures did not increase discrimination to predict all-cause death compared with clinical features.

Myocardial Work and Biomarkers in COVID-19

As mentioned, cardiac injury has been noted as a frequent finding in patients with COVID-19, which was also observed in this study, with 41% exhibiting elevated troponin. Cardiac injury has previously been reported to underly 15% of indications for echocardiography in patients with COVID-19.²⁴ Systolic measures, including both LVEF and GLS, have been shown to be associated with troponin,²⁵ and GLS has been shown to add prognostic information beyond presence of cardiac injury and clinical characteristics.^{26,27} This previously observed additive clinical benefit of echocardiography contrasts with our findings and may

rely on the prior studies being retrospective, with echocardiograms being performed clinically and, hence, subject to indication bias. The strength of a prospective study as ours is that it includes a broader scope of patients with COVID-19, providing more unselected insights as to the pathophysiological features of cardiac injury and myocardial dysfunction. Furthermore, systemic hypertension may itself cause elevations in troponin,^{28,29} and given the after-load dependency of systolic measures, measures seeking to account for BP may therefore be of value to account for this potential underlying confounder and provide a more unbiased assessment of the relationship between troponin and systolic function.

Several mechanisms have been proposed as explanations for why these patients exhibit signs of cardiac injury. First, myocardial injury could indicate ischemia as part of a type 2 myocardial infarction that would reduce the metabolism of the LV.³⁰ This notion is supported by the close correlation between myocardial work and myocardial metabolism that has previously been

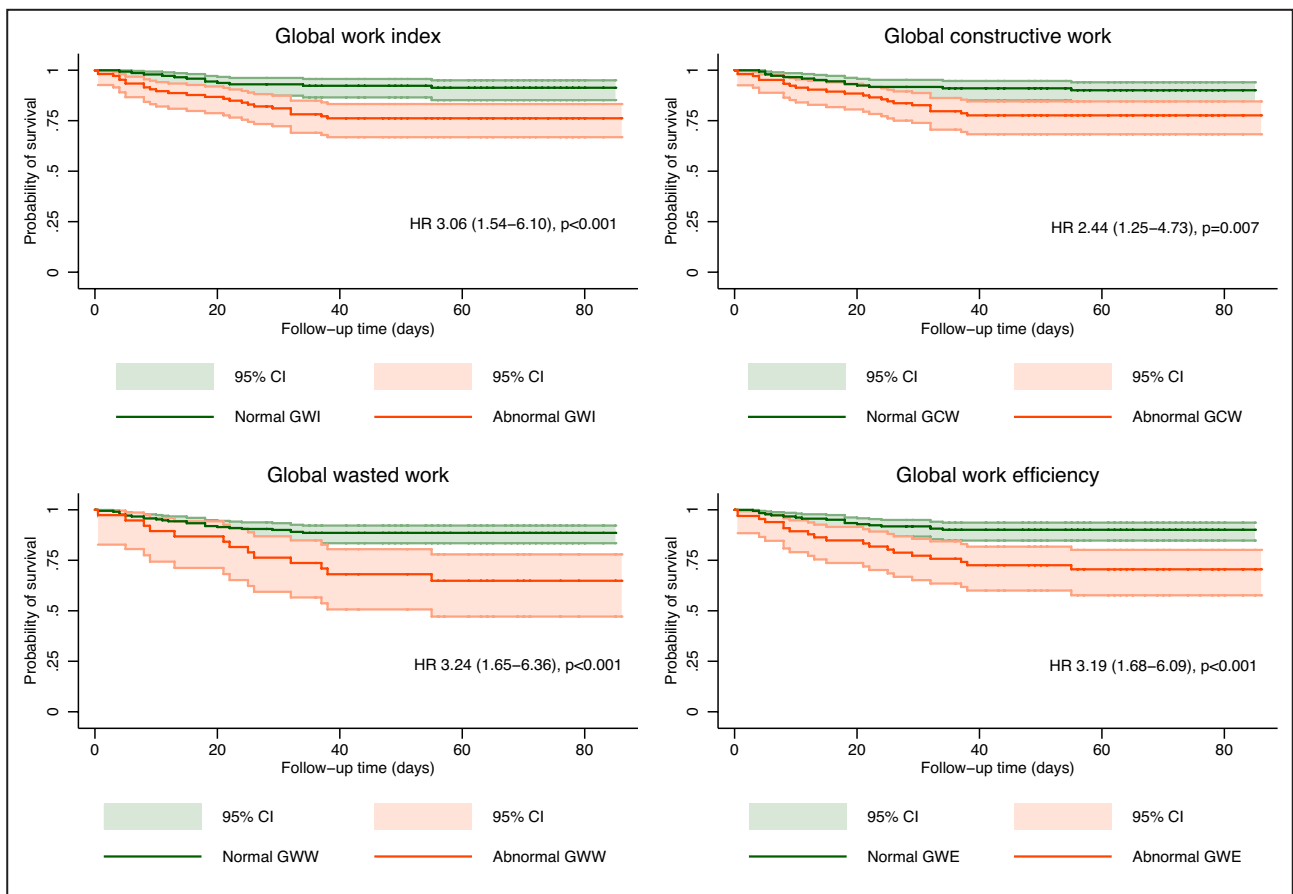


Figure 6. Abnormal work indexes and all-cause death.

The figures represent Kaplan-Meier estimators, showing the probability of survival throughout the follow-up period, according to normal vs abnormal myocardial global work index (GWI) (top left panel), global constructive work (GCW) (top right panel), global wasted work (GWW) (bottom left panel), and global work efficiency (GWE) (bottom right panel).

established,¹² as well as the association we observed between GWI and oxygen requirement. Both GWW and GWE further represent the features of postsystolic shortening and early systolic lengthening, both of which can indicate presence of myocardial ischemia.³¹

However, troponin release could indicate various other conditions, including cytokine storm, myocarditis, stress-induced cardiomyopathy, and myocardial injury secondary to direct viral invasion.⁵ Our findings are in line with a prospective cohort study of patients admitted

Table 2. Continuous Changes in Myocardial Work Indexes and Risk of All-Cause Death

Entire population (n=249; events: 37)					
	Univariable Cox regression			Multivariable Cox regression	
	HR (95% CI)	P value	Harrell' C-statistic	HR (95% CI)	P value
Global work index, per 100-mmHg% decrease	1.14 (1.07–1.21)	<0.001	0.694	1.08 (1.01–1.15)	0.031
Global constructive work, per 100-mmHg% decrease	1.10 (1.04–1.17)	0.002	0.653	1.05 (0.99–1.12)	0.13
Global wasted work, per 50-mmHg% increase	1.15 (1.07–1.23)	<0.001	0.645	1.11 (1.03–1.21)	0.007
Global work efficiency, per % decrease	1.06 (1.03–1.09)	<0.001	0.674	1.04 (1.01–1.08)	0.014
Global longitudinal strain, per % absolute decrease	1.19 (1.10–1.28)	<0.001	0.697	1.10 (1.01–1.19)	0.028

Adjusted for age, early warning score, known heart disease, and left bundle-branch block. HR indicates hazard ratio.

with COVID-19 by Lairez et al (n=31), including patients with abnormal troponin levels, which observed that GWI and GWE were lower in those with abnormal troponin T compared with controls.³² However, in a retrospective cohort study of 136 patients admitted with COVID-19 (PSL available in 75), Minhas et al observed no association between troponin I and measures of LV systolic function, which is at odds with our observation.³³ Of note, this observation should be interpreted in context of the overall normal troponin levels observed in that study, indicating a fairly mild myocardial involvement.

As for troponin, large-scale studies have also noted abnormalities in NT-proBNP that frequently appear in COVID-19 and relate to prognosis, even in the absence of heart failure.³⁴ Although we observed a significant association between GWI and GCW and NT-proBNP, neither Minhas et al nor Lairez et al observed such an association.^{32,33} This discrepancy may rely on the statistical handling, because we observed a nonlinear association, an analytical approach that was not explored in the other studies. Although a stretch-mediated secretion of natriuretic peptides may explain the association between these measures of LV systolic dysfunction and NT-proBNP, as typically observed in heart failure, NT-proBNP is also released as part of the inflammatory response when cytokines are released.³⁵ Accordingly, the association between GWI and GCW and NT-proBNP could therefore also reflect inflammatory burden. This is, however, less likely given that we observed no association between any work indexes and CRP, concordant with other studies.^{32,33}

Clinical Perspective

Although we observed that several work indexes were associated with an increased risk of death, Minhas et al only found GWE to be associated with in-hospital death, whereas no association was observed for GWI, GLS, or LVEF. This underlines the prognostic potential of GWE, whereas the discrepant findings compared with ours may be explained by the smaller sample size and fewer number of events in their study (n=75; events: 25).³³ However, an interesting finding by Minhas et al was that GWE was associated with an increased risk of death even in patients with normal LVEF.³³ Whether there is additional benefit of work indexes compared with GLS has, however, not been clear. In fact, our findings do not suggest superiority of GWI over GLS, but rather that they provide similar prognostic information. Nonetheless, knowing that GLS is influenced by afterload, GWI may serve as a better alternative. Furthermore, GWW, also acquired through PSL analyses, did seem to carry prognostic information independent of GLS. Although this needs to be validated externally, it emphasizes the strength of

PSL analysis in providing a detailed characterization of myocardial tissue function.

Although we observed that work indexes were associated with mortality, they did not improve discrimination for predicting mortality compared with readily available clinical information, including age, EWS, and known heart disease. This defers their routine use in clinical practice, particularly considering the need for limiting exposure time for sonographers.¹ However, in carefully selected patients, echocardiography may change management in up to a third of patients,^{24,36} and the excess mortality observed with myocardial injury and LV dysfunction stresses the need for further studies to clarify the underlying mechanisms to better delineate how biomarkers and echocardiographic measures should be applied clinically to improve prognosis in patients with COVID-19. Furthermore, we did not examine cause-specific death, and it may be possible that work indexes could be clinically useful in terms of improving risk prediction of cardiovascular death. Because RV dysfunction has been reported in 20% of hospitalized patients with COVID-19 and may develop secondary to severe respiratory distress,^{37,38} RV measures may be more valuable in terms of assessing prognosis. Although RV strain has been shown to be associated with mortality, it is also influenced by afterload; and because pulmonary hypertension has similarly been shown to be associated with mortality,³⁹ the prognostic potential of reduced RV strain could therefore be mediated by pulmonary hypertension. Similar to PSL analyses of the LV, RV PSL has recently been proposed as a method to account for RV afterload.^{40,41} Consequently, RV PSL could be of potential use in patients with COVID-19. Although the use of RV PSL may be limited by image quality, particularly in a bedside, short-term setting such as with COVID-19, this could be a point of focus for future studies to clarify the importance of intrinsic RV systolic dysfunction. In addition to outcome prediction, there is also a clinical need to better understand the long-term consequences in patients who recover from COVID-19. Several ailments have been described following COVID-19 infection,⁴² and although RV function has been reported to both improve and deteriorate after recovery of COVID-19 infection, LV function does not seem to improve and may even deteriorate, particularly in moderate-severe infection but also in mild cases.^{43,44} Hence, the consequences of COVID-19 go beyond the immediate infection, and the clinical implications of persistent LV dysfunction need to be explored further.

Strengths and Limitations

Strengths of the study include the large sample size, prospective multicenter design, and protocolized

echocardiographic examination. This is the to date largest echocardiographic study of patients hospitalized with COVID-19.

Several limitations, however, apply to this study. First, the time span between admission and echocardiography of 4 days introduces some bias as patients with COVID-19 who died early after admission would not have been included. Second, patients who did not have PSL analyses performed were older and more frequently had chronic obstructive pulmonary disease, and patients who had NT-proBNP measured more frequently had heart failure at baseline, which suggests some selection bias. We did not include patients from intensive care units. Collectively, these aspects indicate that we cannot generalize our findings to all patients admitted with COVID-19.

Cardiovascular death could have provided different insights as to the prognostic and clinical value of myocardial work indexes; hence, it is a limitation that we did not have information on cause of death in this study.

Because of the low number of events, we were limited as to how many confounders we could adjust for to avoid overfitting. Furthermore, the observational nature of the study also implies that unrecognized and unregistered factors could have influenced the findings, including our lack of details on viral strains of COVID-19. Consequently, there may be residual and uncorrected confounding present in our study. Furthermore, some of our findings may also be ascribed to low statistical power, including the observation that LVEF was not associated with all-cause mortality after multivariable adjustments.

Our analyses on cardiac biomarkers were performed only on a subset of the patients because of missing values; however, the number of covariates that we included in the regression analyses falls within the acceptable number of subjects per variable proposed by simulation studies.⁴⁵ Even so, this warrants caution for the interpretation of our results, and our findings should therefore be validated in larger studies.

CONCLUSIONS

In hospitalized patients with COVID-19, our findings indicate that myocardial work indexes may be associated with troponin and NT-proBNP; however, given the few subjects with available cardiac biomarkers, this should be validated in larger studies. Furthermore, myocardial work indexes are associated with oxygen requirement, but not CRP as a marker of inflammation. Worsening myocardial work indexes posed an increased risk of death in COVID-19; however, the indexes did not improve prognostic assessment when added to readily available clinical details, which does not support their routine use in COVID-19.

ARTICLE INFORMATION

Received May 23, 2022; accepted August 8, 2022.

Affiliations

Department of Cardiology (F.J.O., M.C.H.L., K.G.S., J.C., F.S.D., A.S.A., M.S., A.B.N., N.D.J., M.L., G.G., K.I., M.S., T.B.-S.) and Department of Medicine (P.S., J.U.S.J.), Copenhagen University Hospital - Herlev and Gentofte, Hellerup, Denmark; Department of Biomedical Sciences (F.J.O., A.S.A., M.S., N.D.J., T.B.-S.) and Department of Clinical Medicine (H.B., C.H., O.K., O.W.N., B.L., G.G., K.I., J.U.S.J., M.S., J.H.S.), University of Copenhagen, Copenhagen, Denmark; Department of Cardiology (F.J.O., M.G.L.) and Department of Infectious Diseases (L.W.), Zealand University Hospital, Roskilde, Denmark; Department of Health Science and Technology, Aalborg University, Aalborg, Denmark (C.G.); Department of Cardiology, (H.B., C.H., R.J., J.C., J.H.S.); and Department of Infectious Diseases (O.K.), Copenhagen University Hospital - Rigshospitalet, Copenhagen, Denmark Department of Cardiology, Copenhagen University Hospital - Bispebjerg and Frederiksberg, Copenhagen, Denmark (O.P.K., O.W.N.); Department of Respiratory Medicine and Infectious Diseases (B.L.) and Department of Cardiology (N.T.), Copenhagen University Hospital - North Zealand, Hilleroed, Denmark; Department of Respiratory Medicine, Copenhagen University Hospital - Amager and Hvidovre, Hvidovre, Denmark (C.S.U.); Institute for Surgical Research, Rikshospitalet, Oslo University Hospital and University of Oslo, Oslo, Norway (J.M.A., O.A.S., E.W.R.); and The Intervention Centre, Oslo University Hospital, Rikshospitalet, Oslo, Norway (E.W.R.).

Sources of Funding

The ECHCOVID-19 study was financed by the Novo Nordisk Foundation (grant NFF20SA0062835). Europcar provided a vehicle for transportation between hospitals. Dr Olsen was financed by the Danish Heart Foundation (grant 18-R125-A8534-22083), Herlev and Gentofte Hospital's Research Council, Kong Christian den Tiendes Fond, and Fru Asta Florida Boldings Mindelegat. Dr Biering-Sørensen was funded by Herlev and Gentofte Hospital, Fondsbørsvekslerer Henry Hansen og Hustrus Hovedlegat, the Lundbeck Foundation, and the Novo Nordisk Foundation.

Disclosures

Dr Biering-Sørensen is a Steering Committee member of the Amgen-financed Global Approach to Lowering Adverse Cardiac Outcomes through Improving Contractility in Heart Failure (GALACTIC-HF) trial; is part of the Steering Committee of the Boston Scientific-financed LUX-Dx Heart Failure Sensors in an Insertable Cardiac Monitor System Clinical Study (LUX-Dx TRENDS); is on the Advisory Board of Sanofi Pasteur and Amgen; received speaker honorarium from Novartis and Sanofi Pasteur; and received research grants from GE Healthcare and Sanofi Pasteur. Dr Smiseth is coinventor of the "Method for Myocardial Segment Work Analysis," which was used to calculate myocardial work. Dr Svendsen is on the Advisory Board for Medtronic; received a research grant from Medtronic; and received speaker honorarium from Medtronic. Dr Kirk reports fees for consultation, lectures, and travel by Gilead, Janssen, Merck, and Viiv, outside the submitted work. The remaining authors have no disclosures to report.

Supplemental Material

Data S1
Tables S1-S5
Figure S1

REFERENCES

1. Task Force for the management of COVID-19 of the European Society of Cardiology. European Society of Cardiology guidance for the diagnosis and management of cardiovascular disease during the COVID-19 pandemic: part 1-epidemiology, pathophysiology, and diagnosis. *Eur Heart J*. 2022;43:1033-1058. doi: [10.1093/eurheartj/ehab696](https://doi.org/10.1093/eurheartj/ehab696)
2. Pareek M, Singh A, Vadlamani L, Eder M, Pacor J, Park J, Ghazizadeh Z, Heard A, Cruz-Solbes AS, Nikoobe R, et al. Relation of cardiovascular risk factors to mortality and cardiovascular events in hospitalized patients with coronavirus disease 2019 (from the Yale COVID-19 Cardiovascular Registry). *Am J Cardiol*. 2021;146:99-106. doi: [10.1016/j.amjcard.2021.01.029](https://doi.org/10.1016/j.amjcard.2021.01.029)
3. Figliozzi S, Masci PG, Ahmadi N, Tondi L, Koutli E, Aimo A, Stamatelopoulos K, Dimopoulos M-A, Caforio ALP, Georgiopoulos G.

- Predictors of adverse prognosis in COVID-19: a systematic review and meta-analysis. *Eur J Clin Invest.* 2020;50:e13362. doi: [10.1111/eci.13362](https://doi.org/10.1111/eci.13362)
4. Long B, Brady WJ, Koyfman A, Gottlieb M. Cardiovascular complications in COVID-19. *Am J Emerg Med.* 2020;38:1504–1507. doi: [10.1016/j.ajem.2020.04.048](https://doi.org/10.1016/j.ajem.2020.04.048)
 5. Giustino G, Pinney SP, Lala A, Reddy VY, Johnston-Cox HA, Mechanick JL, Halperin JL, Fuster V. Coronavirus and cardiovascular disease, myocardial injury, and arrhythmia. *J Am Coll Cardiol.* 2020;76:2011–2023. doi: [10.1016/j.jacc.2020.08.059](https://doi.org/10.1016/j.jacc.2020.08.059)
 6. Lala A, Johnson KW, Januzzi JL, Russak AJ, Paranjpe I, Richter F, Zhao S, Somani S, Van Vleck T, Vaid A, et al. Prevalence and impact of myocardial injury in patients hospitalized with COVID-19 infection. *J Am Coll Cardiol.* 2020;76:533–546. doi: [10.1016/j.jacc.2020.06.007](https://doi.org/10.1016/j.jacc.2020.06.007)
 7. Li Y, Li H, Zhu S, Xie Y, Wang B, He L, Zhang D, Zhang Y, Yuan H, Wu C, et al. Prognostic value of right ventricular longitudinal strain in patients with COVID-19. *JACC Cardiovasc Imaging.* 2020;13:2287–2299. doi: [10.1016/j.jcmg.2020.04.014](https://doi.org/10.1016/j.jcmg.2020.04.014)
 8. Lassen MCH, Skaarup KG, Lind JN, Alhakak AS, Sengeløv M, Nielsen AB, Espersen C, Ravnkilde K, Hauser R, Schöps LB, et al. Echocardiographic abnormalities and predictors of mortality in hospitalized COVID-19 patients: the ECHOVID-19 study. *ESC Heart Fail.* 2020;7:4189–4197. doi: [10.1002/ehf2.13044](https://doi.org/10.1002/ehf2.13044)
 9. Stockenhuber A, Vrettos A, Androschuck V, George M, Robertson C, Bowers N, Clifford P, Firoozan S. A pilot study on right ventricular longitudinal strain as a predictor of outcome in COVID-19 patients with evidence of cardiac involvement. *Echocardiography.* 2021;38:222–229. doi: [10.1111/echo.14966](https://doi.org/10.1111/echo.14966)
 10. Wibowo A, Pranata R, Astuti A, Tiksnadi BB, Martanto E, Martha JW, Purnomowati A, Akbar MR. Left and right ventricular longitudinal strains are associated with poor outcome in COVID-19: a systematic review and meta-analysis. *J Intensive Care.* 2021;9:9. doi: [10.1186/s40560-020-00519-3](https://doi.org/10.1186/s40560-020-00519-3)
 11. Khani M, Tavana S, Tabary M, Naseri Kivi Z, Khareshi I. Prognostic implications of biventricular strain measurement in COVID-19 patients by speckle-tracking echocardiography. *Clin Cardiol.* 2021;44:1475–1481. doi: [10.1002/clc.23708](https://doi.org/10.1002/clc.23708)
 12. Russell K, Eriksen M, Aaberge L, Wilhelmsen N, Skulstad H, Remme EW, Haugaa KH, Opdahl A, Fjeld JG, Gjesdal O, et al. A novel clinical method for quantification of regional left ventricular pressure-strain loop area: a non-invasive index of myocardial work. *Eur Heart J.* 2012;33:724–733. doi: [10.1093/eurheartj/ehs016](https://doi.org/10.1093/eurheartj/ehs016)
 13. Lustosa RP, Butcher SC, van der Bijl P, El Mahdiui M, Montero-Cabezas JM, Kostyukevich MV, Rocha De Lorenzo A, Knutti J, Ajmone Marsan N, Bax JJ, et al. Global left ventricular myocardial work efficiency and long-term prognosis in patients after ST-segment-elevation myocardial infarction. *Circ Cardiovasc Imaging.* 2021;14:e012072. doi: [10.1161/CIRCIMAGING.120.012072](https://doi.org/10.1161/CIRCIMAGING.120.012072)
 14. Skaarup KG, Lassen MCH, Lind JN, Alhakak AS, Sengeløv M, Nielsen AB, Espersen C, Hauser R, Schöps LB, Holt E, et al. Myocardial impairment and acute respiratory distress syndrome in hospitalized patients with COVID-19: the ECHOVID-19 study. *JACC Cardiovasc Imaging.* 2020;13:2474–2476. doi: [10.1016/j.jcmg.2020.08.005](https://doi.org/10.1016/j.jcmg.2020.08.005)
 15. Lang RM, Badano LP, Mor-Avi V, Afzalilo J, Armstrong A, Ernande L, Flachskampf FA, Foster E, Goldstein SA, Kuznetsova T, et al. Recommendations for cardiac chamber quantification by echocardiography in adults: an update from the American Society of Echocardiography and the European Association of Cardiovascular Imaging. *J Am Soc Echocardiogr.* 2015;28:1–39.e14. doi: [10.1016/j.echo.2014.10.003](https://doi.org/10.1016/j.echo.2014.10.003)
 16. Galiè N, Humbert M, Vachiery J-L, Gibbs S, Lang I, Torbicki A, Simonneau G, Peacock A, Vonk Noordegraaf A, Beghetti M, et al. 2015 ESC/ERS Guidelines for the diagnosis and treatment of pulmonary hypertension: the Joint Task Force for the Diagnosis and Treatment of Pulmonary Hypertension of the European Society of Cardiology (ESC) and the European Respiratory Society (ERS); endorsed by: Association for European Paediatric and Congenital Cardiology (AEPCC), International Society for Heart and Lung Transplantation (ISHLT). *Eur Heart J.* 2016;37:67–119. doi: [10.1093/eurheartj/ehv317](https://doi.org/10.1093/eurheartj/ehv317)
 17. Biering-Sorensen T. Cardiac time intervals by tissue Doppler imaging M-mode echocardiography: reproducibility, reference values, association with clinical characteristics and prognostic implications. *Dan Med J.* 2016;63:B5279.
 18. Smiseth OA, Donal E, Penicka M, Sletten OJ. How to measure left ventricular myocardial work by pressure-strain loops. *Eur Heart J Cardiovasc Imaging.* 2021;22:259–261. doi: [10.1093/ehjci/jeaa301](https://doi.org/10.1093/ehjci/jeaa301)
 19. Olsen FJ, Skaarup KG, Lassen MCH, Johansen ND, Sengeløv M, Jensen GB, Schnohr P, Marott JL, Søgaard P, Gislason G, et al. Normal values for myocardial work indices derived from pressure-strain loop analyses: from the CCHS. *Circ Cardiovasc Imaging.* 2022;15:e013712. doi: [10.1161/CIRCIMAGING.121.013712](https://doi.org/10.1161/CIRCIMAGING.121.013712)
 20. Wener MH, Daum PR, McQuillan GM. The influence of age, sex, and race on the upper reference limit of serum C-reactive protein concentration. *J Rheumatol.* 2000;27:2351–2359.
 21. Raymond I, Groenning BA, Hildebrandt PR, Nilsson JC, Baumann M, Trawinski J, Pedersen F. The influence of age, sex and other variables on the plasma level of N-terminal pro brain natriuretic peptide in a large sample of the general population. *Heart.* 2003;89:745–751. doi: [10.1136/heart.89.7.745](https://doi.org/10.1136/heart.89.7.745)
 22. Chung MK, Martin DO, Sprecher D, Wazni O, Kanderian A, Carnes CA, Bauer JA, Tchou PJ, Niebauer MJ, Natale A, et al. C-reactive protein elevation in patients with atrial arrhythmias: inflammatory mechanisms and persistence of atrial fibrillation. *Circulation.* 2001;104:2886–2891. doi: [10.1161/hc4901.101760](https://doi.org/10.1161/hc4901.101760)
 23. Panichi V, Migliori M, De Pietro S, Taccola D, Bianchi AM, Norpoth M, Metelli MR, Giovannini L, Tetta C, Palla R. C reactive protein in patients with chronic renal diseases. *Ren Fail.* 2001;23:551–562. doi: [10.1081/JDI-100104737](https://doi.org/10.1081/JDI-100104737)
 24. Jain SS, Liu Q, Raikhelkar J, Fried J, Elias P, Poterucha TJ, DeFilippis EM, Rosenblum H, Wang EY, Redfors B, et al. Indications for and findings on transthoracic echocardiography in COVID-19. *J Am Soc Echocardiogr.* 2020;33:1278–1284. doi: [10.1016/j.echo.2020.06.009](https://doi.org/10.1016/j.echo.2020.06.009)
 25. Bagate F, Masi P, d'Humières T, Al-Assaad L, Chakra LA, Razaki K, de Prost N, Carreaux G, Derumeaux G, Mekontso Dessap A. Advanced echocardiographic phenotyping of critically ill patients with coronavirus-19 sepsis: a prospective cohort study. *J Intensive Care.* 2021;9:12. doi: [10.1186/s40560-020-00516-6](https://doi.org/10.1186/s40560-020-00516-6)
 26. Sun W, Zhang Y, Wu C, Xie Y, Peng L, Nie X, Yu C, Zheng Y, Li Y, Wang J, et al. Incremental prognostic value of biventricular longitudinal strain and high-sensitivity troponin I in COVID-19 patients. *Echocardiography.* 2021;38:1272–1281. doi: [10.1111/echo.15133](https://doi.org/10.1111/echo.15133)
 27. Pournazari P, Spangler AL, Ameer F, Hagan KK, Tano ME, Chamsi-Pasha M, Chebrolu LH, Zoghbi WA, Nasir K, Nagueh SF. Cardiac involvement in hospitalized patients with COVID-19 and its incremental value in outcomes prediction. *Sci Rep.* 2021;11:19450. doi: [10.1038/s41598-021-98773-4](https://doi.org/10.1038/s41598-021-98773-4)
 28. Acosta G, Amro A, Aguilar R, Abusnina W, Bhardwaj N, Koromia GA, Studeny M, Irfan A. Clinical determinants of myocardial injury, detectable and serial troponin levels among patients with hypertensive crisis. *Cureus.* 2020;12:e6787. doi: [10.7759/cureus.6787](https://doi.org/10.7759/cureus.6787)
 29. Koracevic GP. Among numerous causes of high troponin values, we should not forget severe arterial hypertension. *Am J Emerg Med.* 2021;46:794–795. doi: [10.1016/j.ajem.2020.08.063](https://doi.org/10.1016/j.ajem.2020.08.063)
 30. Thygesen K, Alpert JS, Jaffe AS, Chaitman BR, Bax JJ, Morrow DA, White HD; Executive Group on behalf of the Joint European Society of Cardiology (ESC)/American College of Cardiology (ACC)/American Heart Association (AHA)/World Heart Federation (WHF) Task Force for the Universal Definition of Myocardial Infarction. Fourth Universal Definition of Myocardial Infarction (2018). *Circulation.* 2018;138:e618–e651. doi: [10.1161/CIR.0000000000000617](https://doi.org/10.1161/CIR.0000000000000617)
 31. Brainin P. Myocardial postsystolic shortening and early systolic lengthening: current status and future directions. *Diagnostics.* 2021;11:1428. doi: [10.3390/diagnostics11081428](https://doi.org/10.3390/diagnostics11081428)
 32. Lairez O, Blanchard V, Houard V, Vardon-Bouines F, Lemasle M, Cariou E, Lavie-Badie Y, Ruiz S, Cazalbou S, Delmas C, et al. Cardiac imaging phenotype in patients with coronavirus disease 2019 (COVID-19): results of the cocarde study. *Int J Cardiovasc Imaging.* 2021;37:449–457. doi: [10.1007/s10554-020-02010-4](https://doi.org/10.1007/s10554-020-02010-4)
 33. Minhas AS, Gilotra NA, Goerlich E, Metkus T, Garibaldi BT, Sharma G, Bavaro N, Phillip S, Michos ED, Hays AG. Myocardial work efficiency, a novel measure of myocardial dysfunction, is reduced in COVID-19 patients and associated with in-hospital mortality. *Front Cardiovasc Med.* 2021;8:667721. doi: [10.3389/fcvm.2021.667721](https://doi.org/10.3389/fcvm.2021.667721)
 34. Caro-Codón J, Rey JR, Buño A, Iniesta AM, Rosillo SO, Castrejon-Castrejon S, Rodriguez-Sotelo L, Martinez LA, Marco I, Merino C, et al. Characterization of NT-proBNP in a large cohort of COVID-19 patients. *Eur J Heart Fail.* 2021;23:456–464. doi: [10.1002/ejhf.2095](https://doi.org/10.1002/ejhf.2095)
 35. Goetze JP, Bruneau BG, Ramos HR, Ogawa T, de Bold MK, de Bold AJ. Cardiac natriuretic peptides. *Nat Rev Cardiol.* 2020;17:698–717. doi: [10.1038/s41569-020-0381-0](https://doi.org/10.1038/s41569-020-0381-0)

36. Dweck MR, Bularga A, Hahn RT, Bing R, Lee KK, Chapman AR, White A, Salvo GD, Sade LE, Pearce K, et al. Global evaluation of echocardiography in patients with COVID-19. *Eur Heart J Cardiovasc Imaging*. 2020;21:949–958. doi: [10.1093/ehjci/jeaa178](https://doi.org/10.1093/ehjci/jeaa178)
37. Corica B, Marra AM, Basili S, Cangemi R, Cittadini A, Proietti M, Romiti GF. Prevalence of right ventricular dysfunction and impact on all-cause death in hospitalized patients with COVID-19: a systematic review and meta-analysis. *Sci Rep*. 2021;11:17774. doi: [10.1038/s41598-021-96955-8](https://doi.org/10.1038/s41598-021-96955-8)
38. Repessé X, Vieillard-Baron A. Right heart function during acute respiratory distress syndrome. *Ann Transl Med*. 2017;5:295. doi: [10.21037/atm.2017.06.66](https://doi.org/10.21037/atm.2017.06.66)
39. Pagnesi M, Baldetti L, Beneduce A, Calvo F, Gramegna M, Pazzanese V, Ingallina G, Napolano A, Finazzi R, Ruggeri A, et al. Pulmonary hypertension and right ventricular involvement in hospitalised patients with COVID-19. *Heart*. 2020;106:1324–1331. doi: [10.1136/heartjnl-2020-317355](https://doi.org/10.1136/heartjnl-2020-317355)
40. Richter MJ, Yogeswaran A, Husain-Syed F, Vadász I, Rako Z, Mohajerani E, Ghofrani HA, Naeije R, Seeger W, Herberg U, et al. A novel non-invasive and echocardiography-derived method for quantification of right ventricular pressure-volume loops. *Eur Heart J Cardiovasc Imaging*. 2021;23:498–507. doi: [10.1093/ehjci/jeab038](https://doi.org/10.1093/ehjci/jeab038)
41. Smiseth OA, Aalen JM. Right ventricular work: a step forward for non-invasive assessment of right ventricular function. *Eur Heart J Cardiovasc Imaging*. 2021;22:153–154. doi: [10.1093/ehjci/jeaa296](https://doi.org/10.1093/ehjci/jeaa296)
42. Lopez-Leon S, Wegman-Ostrosky T, Perelman C, Sepulveda R, Rebolledo PA, Cuapio A, Villapol S. More than 50 long-term effects of COVID-19: a systematic review and meta-analysis. *Sci Rep*. 2021;11:16144. doi: [10.1038/s41598-021-95565-8](https://doi.org/10.1038/s41598-021-95565-8)
43. Chaturvedi H, Issac R, Sharma SK, Gupta R. Progressive left and right heart dysfunction in coronavirus disease-19: prospective echocardiographic evaluation. *Eur Heart J Cardiovasc Imaging*. 2022;23:319–325. doi: [10.1093/ehjci/jeab268](https://doi.org/10.1093/ehjci/jeab268)
44. Lassen MCH, Skaarup KG, Lind JN, Alhakak AS, Sengeløv M, Nielsen AB, Simonsen JØ, Johansen ND, Davidovski FS, Christensen J, et al. Recovery of cardiac function following COVID-19 - ECHOVID-19: a prospective longitudinal cohort study. *Eur J Heart Fail*. 2021;23:1903–1912. doi: [10.1002/ejhf.2347](https://doi.org/10.1002/ejhf.2347)
45. Austin PC, Steyerberg EW. The number of subjects per variable required in linear regression analyses. *J Clin Epidemiol*. 2015;68:627–636. doi: [10.1016/j.jclinepi.2014.12.014](https://doi.org/10.1016/j.jclinepi.2014.12.014)

SUPPLEMENTAL MATERIAL

Data S1.

Supplemental Methods

Definition of comorbidities

Hypertension was defined as self-reported condition, use of antihypertensive medication, or reported condition in the medical records. Diabetes mellitus was similarly defined as self-reported condition, use of antidiabetic medication, or reported condition in the medical records. Heart failure was also defined as self-reported condition, use of relevant medication for the indication of heart failure (beta blocker, RAAS-inhibitors, aldosterone antagonist), or reported condition in the medical records. Known ischemic heart disease was defined as prior admission with acute myocardial infarction, percutaneous coronary intervention, or coronary artery bypass grafting.

Conventional echocardiographic analyses

LV dimensions were measured from the parasternal long-axis view and used to calculate left ventricular (LV) mass index (Devereux' formula), which was indexed to body surface area (DuBois' formula). LV ejection fraction was measured by the Simpson's biplane method. Tricuspid annular plane systolic excursion was measured by M-mode through the tricuspid annulus from the apical 4-chamber view. The peak tricuspid regurgitant (TR) velocity was measured with continuous wave Doppler placed perpendicularly through a TR jet if present (n=189). RV hypertension was defined according to RV hypertension guidelines as a TR velocity > 2.8 m/s. If TR was not measurable, presence of right ventricular (RV) hypertension was based on secondary indicators, including D-shape of the LV, RV-LV diameter ratio, pulmonary outflow velocity, right atrial area, and inferior vena cava size and collapse.

Abnormal work indices

Abnormal work indices were defined according to previously established reference values based on data from the Copenhagen City Heart Study.

Abnormal global work index (GWI) was defined as a GWI < 1534 mmHg% for men. For women, abnormal GWI was defined as a GWI < 1604 mmHg% for age < 40 years, a GWI < 1646 mmHg% for age of 40-60 years, and a GWI < 1599 mmHg% for age > 60 years.

For men, abnormal global constructive work (GCW) was defined as a GCW < 1715 mmHg% for age < 40 years, a GCW < 1671 mmHg% for age of 40-60 years, and GCW < 1691 mmHg% for age > 60

years. For women, abnormal GCW was defined as a GCW<1706 mmHg% for age<40 years, a GCW<1754 mmHg% for age of 40-60 years, and a GCW<1759 mmHg% for age>60 years.

Abnormal global wasted work (GWW) was defined as a GWW>153 mmHg% for men. For women, abnormal GWW was defined as a GWW>145 mmHg% for age<40 years, a GWW>167 mmHg% for age of 40-60 years, and a GWW>199 mmHg% for age>60 years.

Abnormal global work efficiency (GWE) was defined as a GWE<93.2% for men. For women, abnormal GWE was defined as a GWE<93.6% for age<40 years, a GWE<92.9% for age of 40-60 years, and a GWE<90.6% for age>60 years.

Table S1 – Clinical characteristics across the two ECHOVID waves

	1 st COVID-19 wave n=215	2 nd COVID-19 wave n=90	p-value
Age, years	69±14	70±16	0.59
Male sex	118 (55)	56 (62)	0.24
Body mass index, kg/m ²	27±6	27±5	0.85
Systolic blood pressure, mmHg	126±19	129±19	0.30
Diastolic blood pressure, mmHg	73±11	74±12	0.25
Heart rate, bpm	80±17	82±17	0.43
Oxygen saturation, %	95 [94;97]	94 [93;97]	0.20
Respiratory rate	19 [18;20]	18 [16;20]	0.48
Temperature, °C	37.1±0.68	36.9 ±0.72	0.013
Hypertension, n (%)	106 (49)	54 (60)	0.09
Diabetes mellitus, n (%)	57 (27)	23 (26)	0.83
COPD, n (%)	32 (15)	17 (19)	0.38
Ischemic heart disease, n (%)	20 (9)	15 (17)	0.06
Heart failure, n (%)	22 (10)	12 (13)	0.43
Supplemental oxygen, L/min	1 [0;3]	1 [0;2]	0.52
Plasma C-reactive protein, mg/L	58 [25;98]	39 [21;76]	0.037

COPD: chronic obstructive pulmonary disease

Table S2 – Clinical characteristics by feasibility

	PSL not feasible n=56	PSL feasible n=249	p-value
Age, years	73±13	68±14	0.026
Male sex	31 (55)	143 (57)	0.78
Body mass index, kg/m ²	27±6	27±5	0.53
Systolic blood pressure, mmHg	128±20	127±19	0.62
Diastolic blood pressure, mmHg	71±12	74±11	0.16
Heart rate, bpm	80±19	81±16	0.65
Oxygen saturation, %	95 [93;97]	95 [94;96]	0.70
Respiratory rate	20 [18;24]	18 [17;20]	0.12
Temperature, °C	37.0±0.73	37.0 ±0.69	0.65
Hypertension, n (%)	29 (52)	131 (53)	0.91
Diabetes mellitus, n (%)	18 (32)	62 (25)	0.28
COPD, n (%)	16 (29)	33 (13)	0.005
Ischemic heart disease, n (%)	9 (17)	26 (10)	0.19
Heart failure, n (%)	9 (16)	25 (10)	0.20

COPD: chronic obstructive pulmonary disease

Table S3- Baseline characteristics according to myocardial injury

	No cardiac injury n=103	Cardiac injury n=71	p-value
Clinical			
Age, years	65±14	74±13	<0.001
Male sex	58 (56)	40 (56)	1.00
Body mass index, kg/m ²	27±6	26±5	0.47
Early warning score	2 [1;3]	2 [1;4]	0.45
Systolic blood pressure, mmHg	126±20	127±19	0.79
Diastolic blood pressure, mmHg	74±11	72±11	0.26
Heart rate, beats/minute	80±15	81±17	0.78
Oxygen saturation, %	95 [94;96]	95 [93;97]	0.71
Respiratory rate	18 [16;20]	18 [18;22]	0.33
Temperature, °C	37.0±0.67	37.0±0.67	0.74
Hypertension, n (%)	52 (51)	47 (66)	0.040
Diabetes mellitus, n (%)	27 (26)	17 (14)	0.78
Chronic obstructive pulmonary disease, n (%)	10 (10)	14 (20)	0.06
Ischemic heart disease, n (%)	7 (7)	11 (16)	0.06
Heart failure, n (%)	5 (5)	15 (21)	<0.001
Biomarkers			
Plasma Pro-brain natriuretic peptide, ng/L	220 [102;699]	751 [377;1522]	<0.001
Plasma C-reactive protein, mg/L	58 [23;89]	56 [24;97]	0.41
Plasma Creatinine, µmol/L	70 [56;88]	92 [64;134]	<0.001
Echocardiography			
Left ventricular mass index, g/m ²	78 [66;94]	90 [73;115]	0.030
Left ventricular internal diameter, cm	4.5±0.7	4.6±0.7	0.17
Left ventricular ejection fraction, %	60 [54;64]	56 [51;62]	0.024
Left atrial volume, mL/m ²	21 [15;25]	19 [15;30]	0.76
Tricuspid annular plane systolic excursion, mm	21±4.9	20±4.6	0.09
Tricuspid regurgitant gradient, mmHg	21±10	23±8	0.35
Right ventricular hypertension, n (%)	16 (16)	10 (14)	0.79
Global longitudinal strain, %	-16.1±3.9	14.4±4.3	0.007
Global work index, mmHg%	1707±542	1508±536	0.018
Global constructive work, mmHg%	1887±542	1701±531	0.026
Global wasted work, mmHg%	81 [50;132]	81 [54;142]	0.35
Global work efficiency, %	95.8 [92.8;97.2]	95.1 [89.9;97.2]	0.11

Continuous variables showing Gaussian distribution are shown as mean ± standard deviation. Continuous variables not showing Gaussian distribution are shown as median with [interquartile range].

Table S4 – Clinical characteristics by BNP measurement

	BNP not measured n=87	BNP measured n=162	p-value
Age, years	67±14	69±14	0.55
Male sex	47 (54)	96 (59)	0.43
Body mass index, kg/m ²	27±5	27±6	0.99
Systolic blood pressure, mmHg	126±17	127±20	0.91
Diastolic blood pressure, mmHg	75±12	73±11	0.18
Heart rate, bpm	82±16	81±16	0.64
Oxygen saturation, %	95 [94;96]	95 [93;96]	0.30
Respiratory rate	18 [17;20]	18 [18;20]	0.38
Temperature, °C	37.1±0.75	37.0 ±0.65	0.33
Hypertension, n (%)	45 (52)	86 (53)	0.84
Diabetes mellitus, n (%)	25 (29)	37 (23)	0.26
COPD, n (%)	9 (10)	24 (15)	0.32
Ischemic heart disease, n (%)	10 (12)	16 (10)	0.69
Heart failure, n (%)	4 (5)	21 (13)	0.045

BNP: brain-natriuretic peptide; COPD: chronic obstructive pulmonary disease

Table S5 - Baseline characteristics according to all-cause death

	Alive n=212	Deceased n=37	p-value
Clinical			
Age, years	66±14	78±9	<0.001
Male sex	116 (55)	27 (73)	0.038
Body mass index, kg/m ²	27±6	25±5	0.046
Early warning score	2 [1;3]	3 [2;4]	0.002
Systolic blood pressure, mmHg	127±19	124±18	0.30
Diastolic blood pressure, mmHg	74±11	72±14	0.34
Heart rate, beats/minute	80±15	88±22	0.002
Oxygen saturation, %	95 [94;96]	94 [92;97]	0.29
Respiratory rate	18 [17;20]	20 [18;24]	0.07
Temperature, °C	37.1±0.68	37.0±0.73	0.90
Hypertension, n (%)	106 (50)	25 (68)	0.048
Diabetes mellitus, n (%)	55 (26)	7 (19)	0.35
Chronic obstructive pulmonary disease, n (%)	24 (11)	9 (24)	0.031
Ischemic heart disease, n (%)	20 (9)	6 (16)	0.21
Heart failure, n (%)	17 (8)	9 (24)	0.002
Biomarkers			
Plasma Pro-brain natriuretic peptide, ng/L	313 [110;1285]	506 [228;3061]	0.048
Plasma Troponin I, ng/L	11 [7;25]	35 [18;49]	<0.001
Plasma Troponin T, ng/L	19 [13;32]	35 [21;118]	0.007
Plasma C-reactive protein, mg/L	46 [19;81]	93 [62;146]	<0.001
Plasma Creatinine, μmol/L	72 [57;93]	109 [64;194]	<0.001
Echocardiography			
Left ventricular mass index, g/m ²	81 [69;95]	92 [61;115]	0.65
Left ventricular internal diameter, cm	4.5±0.7	4.4±0.8	0.26
Left ventricular ejection fraction, %	59 [54;63]	54 [42;61]	0.009
Tricuspid annular plane systolic excursion, mm	21±5	18±5	0.002
Tricuspid regurgitant gradient, mmHg	21±9	23±9	0.35
Right ventricular hypertension, n (%)	25 (12)	7 (19)	0.23
Global work index, mmHg%	1717±523	1329±592	<0.001
Global constructive work, mmHg%	1898±556	1585±565	0.002
Global wasted work, mmHg%	70 [44;123]	111 [68;233]	<0.001
Global work efficiency, %	95.9 [92.9;97.6]	91.5 [86.4;96.4]	<0.001

Continuous variables showing Gaussian distribution are shown as mean ± standard deviation. Continuous variables not showing Gaussian distribution are shown as median with [interquartile range].

Figure S1. C-reactive protein according to normal vs. abnormal work indices.

Bar charts showing no significant differences in the concentration of CRP according to normal vs. abnormal myocardial work indices.

CRP: C-reactive protein

